JACC: CARDIOVASCULAR IMAGING
VOL. 8, NO. 11, 2015

ISSN 1936-878X/$36.00
PUBLISHED BY ELSEVIER INC.
http://dx.doi.org/10.1016/j.jcmg.2015.09.003

Functional Evaluation of Coronary Disease by CT Angiography

Pedro de Araújo Gonçalves, MD, PhD,* Gastón A. Rodríguez-Granillo, MD, PhD,† Ernest Spitzer, MD,‡ Pannipa Suwannasom, MD,§ Christian Loewe, MD,‖ Koen Nieman, MD, PhD,¶ Hector M. Garcia-Garcia, MD, PhD‡§

ABSTRACT

In recent years, several technical developments in the field of cardiac computed tomography (CT) have made possible the extraction of functional information from an anatomy-based examination. Several different lines have been explored and will be reviewed in the present paper, namely: 1) myocardial perfusion imaging; 2) transluminal attenuation gradients and corrected coronary opacification indexes; 3) fractional flow reserve computed from CT; and 4) extrapolation from atherosclerotic plaque characteristics. In view of these developments, cardiac CT has the potential to become in the near future a truly 2-in-1 noninvasive evaluation for coronary artery disease. (J Am Coll Cardiol Img 2015;8:1322–35)

Less than 10 years have passed since the publication of the first studies reporting on the diagnostic performance of the 64-slice scanners, which led to the wide adoption of cardiac computed tomography (CT) in clinical practice (1,2), and we are still witnessing impressive technical improvements in this field. These advances have led to significant improvements in temporal resolution and volume coverage and associated reductions in scan time, contrast, and radiation dose, which have made possible the progressive development of protocols aimed at extracting functional information about coronary artery disease (CAD) lesions. This is of utmost importance because clinical decision making, namely the decision to proceed to a revascularization procedure, is based on the expected functional effect of CAD lesions, as it has been well documented that there is no prognostic benefit of revascularization in the absence of functional significance (3–5). Several noninvasive diagnostic tools are already readily available, from the simple exercise electrocardiogram (ECG) to stress echocardiography, single-photon emission computed tomography (SPECT), and stress cardiac magnetic resonance imaging (CMR), and their use in clinical practice is influenced by several different factors related not only to their diagnostic performance, but also to availability and patient-related features (6). The potential advantage of cardiac CT in this field comes from both its wide clinical adoption in recent years and the attractive concept of having a 2-in-1 examination, providing anatomic plus functional CAD evaluation. In this concept, cardiac CT might be able to not only rule out CAD with a very high accuracy, but also provide additional functional information in case CAD is documented, moving beyond the usual classification of *obstructive versus nonobstructive* to a more functional-based interpretation of *significant versus nonsignificant* CAD, a feature that is linked more closely to the current clinical decision algorithm.

MYOCARDIAL PERFUSION IMAGING

The diagnostic accuracy and prognostic value of cardiac CT in patients with low to intermediate CAD likelihood has been largely established. Nevertheless, the performance of this technique in patients with intermediate to high CAD likelihood has been associated

From the *Hospital de Santa Cruz, Hospital da Luz, and CEDOC-Nova Medical School, Lisbon, Portugal; †Department of Cardiovascular Imaging, Diagnostico Maipu, and Consejo Nacional de Investigaciones Cientificas y Tecnicas (CONICET), Buenos Aires, Argentina; ‡Cardialysis B.V., Rotterdam, the Netherlands; §Thoraxcenter, Erasmus Medical Center, Rotterdam, the Netherlands; ‖Section of Cardiovascular and Interventional Radiology, Department of Bioimaging and Image-Guided Therapy, Medical University of Vienna, Vienna, Austria; and the ¶Departments of Cardiology and Radiology, Erasmus Medical Center, Rotterdam, the Netherlands. Dr. Nieman has received institutional research support from Siemens Medical Solutions, GE Healthcare, and Bayer Healthcare. All other authors have reported that they have no relationships relevant to the contents of this paper to disclose.

Manuscript received July 18, 2015; revised manuscript received August 30, 2015, accepted September 3, 2015.

with a low specificity. The major advantage of coronary computed tomographic angiography (CTA) lies in a very high negative predictive value, which rules out CAD with high reliability. However, the positive predictive value of the test is not sufficiently high, ascribed to a relatively high false positive rate in selected populations (7). This is mainly due to the presence of artifacts (i.e., blooming, beam hardening) related to coronary calcification in the setting of the still limited spatial resolution of this technique (8). The presence of heavy, particularly concentric, calcification hampers the clear visualization of lumen and its distinction from atherosclerotic plaque, occasionally resulting in false positive findings and/or inconclusive studies, and thus leading to potential unnecessary referral to invasive coronary angiography (ICA) or to further diagnostic tests. Overall, these limitations broaden the spectrum of restrictions of the technique in addition to other exclusion criteria, such as patients with arrhythmia and inability to achieve target heart rate (due to motion artifacts) and patients at risk of contrast-induced nephropathy.

However, the fact that obstructive lesions identified by cardiac CT have demonstrated a weak correlation with the presence of ischemia underscores the need for a hemodynamic assessment in addition to the anatomic evaluation (9,10).

Despite recent conflicting findings from a subanalysis of the COURAGE (Clinical Outcomes Utilizing Revascularization and Aggressive Drug Evaluation) and STICH (Surgical Treatment for Ischemic Heart Failure) trials, which have casted some doubts regarding the prognostic value of inducible ischemia as the sole indicator of revascularization, clinical decision making remains linked to the presence or absence of myocardial ischemia, given the largely established prognostic value of stress myocardial perfusion imaging (11,12). Furthermore, the estimation of the physiological effect of a given epicardial obstruction (particularly of intermediate lesions) is highly relevant to determining a treatment strategy, independently of the pre-test CAD likelihood.

Overall, the previously mentioned shortcomings have set the foundation for major technical developments achieved during the past decade, aimed at evaluating the functional significance of coronary stenosis by means of cardiac CT. One of the emerging strategies in this regard is CT myocardial perfusion imaging (MPI) under pharmacological stress, a technique that is positioned as the only tool capable of detecting a stenosis, which establishes its hemodynamic significance. Two different approaches are available for CT-MPI: static or dynamic (**Table 1**).

Static CT-MPI acquisitions comprise the evaluation of myocardial perfusion obtained from a single dataset acquired during first-pass enhancement and enable a qualitative assessment of differences in contrast enhancement based on myocardial perfusion (13–15). In this approach, attenuation levels of the ischemic areas are compared with the signal density of the remote (normal) myocardium areas. Accordingly, patients with balanced myocardial ischemia may not be easily identified using this technique, although it is noteworthy that diffuse ischemia might be identified as a myocardium with homogeneously low myocardial attenuation levels. In parallel, peak myocardial attenuation may be missed if bolus timing is not accurate, thus potentially affecting the ability to discriminate between normal and ischemic regions (16).

However, dynamic CT-MPI provides a quantitative estimation of myocardial time-attenuation curves and other parameters such as myocardial blood flow (MBF) (17–21). The concept of dynamic CT-MPI is based on the evaluation of multiple sequential CT datasets of myocardial attenuation levels after the injection of a contrast bolus, enabling the generation of time-attenuation curves during arrival and washout of contrast to and from the myocardium and aorta over time. Quantification of absolute MBF using this technique has been validated in animal models using variable degrees of coronary stenosis, showing a good correlation between CT-MBF and coronary blood flow as well as between CT-MBF and fractional flow reserve (FFR) (22,23). Several clinical studies have been conducted aiming to assess absolute quantification of MBF using stress dynamic CT-MPI in humans (21,24,25). Indeed, cutoff points between 75 and 78 ml/100 ml/min have been proposed as the optimal threshold values for the discrimination between significant and nonsignificant lesions (21,26).

The core limitation of dynamic CT-MPI is a significantly increased radiation dose compared with static CT-MPI, as well as the need for longer breath-holding that warrants the use of further motion correction algorithms (27,28). Indeed, effective radiation dose of dynamic CT-MPI using 128-detector dual-source scanners has been reported to range between 9.2 and 12.5 mSv (28). Moreover, a number of studies have suggested that MBF measurements might be slightly underestimated by dynamic CT-MPI (24,29).

Static CT-MPI demands an additional scan to conventional coronary CTA protocol; thereby, radiation

ABBREVIATIONS AND ACRONYMS

CAD = coronary artery disease

CCO = corrected coronary opacification

CMR = cardiac magnetic resonance

CT = computed tomography

CTA = computed tomography angiography

FFR = fractional flow reserve

HU = Hounsfield units

ICA = invasive coronary angiography

MBF = myocardial blood flow

MPI = myocardial perfusion imaging

SPECT = single-photon emission computed tomography

TAG = transluminal attenuation gradients

exposure of this approach is directly related to the acquisition mode. Although acquisitions using 128-slice dual-source high-pitch CT-MPI have been reported to achieve a radiation exposure of only 2.5 mSv for the entire stress/rest CT protocol, this has not been replicated in other studies (30).

It is noteworthy that both approaches (static and dynamic CT-MPI) have shown a high diagnostic performance for the detection of perfusion defects, and a recent study has shown a good agreement between both methods (31).

The aim of stress CT-MPI is to complement coronary CTA findings during a single procedure. Numerous single-center studies have validated this application using different scanners, pharmacological agents (adenosine, dipyridamole, and regadenoson), and acquisition protocols (14,15,17–19,30–33). Overall, these studies showed good agreement between stress CT-MPI and SPECT, ICA, and/or stress CMR, with the obvious advantage of providing additional information regarding the presence and extent of underlying coronary obstruction. Indeed, most of the aforementioned studies indicated that the addition of stress CT-MPI provides a significant incremental value over anatomic evaluation alone by coronary CTA for the detection of reversible perfusion defects. Stress CMR is currently considered the noninvasive reference standard in terms of MPI, and CT-MPI has demonstrated a 86% sensitivity, 98% specificity, 94% positive predictive value, and 96% negative predictive value for the detection of perfusion defects compared with CMR (33). Stress CT-MPI has also been recently compared to FFR, showing that in territories where coronary CTA and CT-MPI are concordant, the combined evaluation is highly accurate in the detection and exclusion of ischemia (32). In that study, the specificity and positive predictive value increased from 84% to 98% and from 82% to 97%, respectively, after adding CT-MPI to CTA.

A recently published multicenter study (CORE320 [Coronary Artery Evaluation using 320-row Multidetector Computed Tomography Angiography and Myocardial Perfusion]) has confirmed earlier findings on a larger scale. In this study, the overall performance of CT-MPI in the diagnosis of obstructive CAD was higher than that of SPECT. Whereas SPECT demonstrated a higher specificity, CT-MPI showed a higher sensitivity, partly due to the higher sensitivity for left main and multivessel disease assessment (34). It should be noted that the reference used in this study was a conservative anatomic threshold of 50% stenosis by ICA. More recently, a randomized, multicenter, multivendor study demonstrated noninferiority of regadenoson CT-MPI compared with SPECT for the detection of myocardial ischemia, with an agreement rate of 0.87 (95% confidence interval [CI]: 0.77 to 0.97). In this study, the diagnostic accuracy of CT-MPI and coronary CTA alone were 0.85 (95% CI: 0.78 to 0.91) and 0.69 (95% CI: 0.60 to 0.77), respectively (35).

As previously mentioned, static CT-MPI requires 2 scans: 1 with pharmacological stress and the other during rest (**Figure 1**). In general, retrospective ECG gating is used for stress acquisitions with tube current modulation aimed at decreasing radiation dose as low as possible. Retrospective acquisitions are less susceptible to artifacts related to increased and/or irregular heart rate and allow the possibility of having systolic and diastolic phases that aid the discrimination between motion artifacts and perfusion defects. Rest scans are usually performed in prospective mode to achieve the lowest radiation dose. Overall, this combined scan allows the simultaneous evaluation of coronary anatomy as well as the functional significance of CAD by assessing myocardial perfusion after hyperemia. Myocardial perfusion defects, identified by hypoenhanced areas, can be reversible (ischemia) or fixed (scar). If needed, a third noncontrast scan can be added to confirm the presence of scar (delayed-enhancement) attributed mainly to an expansion in the extracellular volume, which has been shown to predict clinical outcome in patients with acute myocardial infarction (36,37). This scan can be performed in a prospective mode using a very low radiation dose. Nevertheless, chronic infarct sizes evaluated by delayed-enhancement CT are significantly smaller than those from matching CMR (38). It is also worth mentioning that CT and magnetic resonance, as opposed to SPECT, provide an evaluating of transmural extension, with a potential advantage for CT due to a lower contrast-to-noise ratio (39).

In the past few years, there has been a growing interest in the development of a noninvasive "1-stop shop" tool that can evaluate in a single session both coronary anatomy and the presence of ischemia. The spectrum of patients who might be eligible for cardiac CT might be widened by eventually including patients who were formerly excluded from most protocols, such as patients outside of the borders of intermediate CAD probability. Indeed, it is expected that in the future, the order or extent of the scan might be selected according to the pre-test CAD likelihood (anatomy [rest] only, anatomy with eventual perfusion [rest plus stress], stress-perfusion, and stress-perfusion plus delayed-enhancement). Actually, technical developments such as faster gantry rotation speed and intracycle motion correction

algorithms aid the attenuation of artifacts related to high or irregular heart rates and, therefore, might lead in the future to an accurate assessment of the coronary tree with stress-only acquisitions, thus further saving radiation dose (40). The issue of radiation is of utmost importance when faced with other functional modalities that do not require ionizing radiation, like stress CMR and stress echocardiography, but in recent years, several hardware (e.g., dual-source, high-volume coverage, more powerful Roentgen tubes, dedicated filters) and software (e.g., low Kv scanning, prospective ECG-gated scan protocols, iterative reconstruction techniques) developments have led to an impressive reduction in cardiac CT radiation dose (41).

One of the potential applications of CT-MPI is in the triage of patients with acute chest pain. Rest CT-MPI evaluated concurrently during routine cardiac CT shows promise in detection of perfusion defects in the presence of acute coronary occlusion (42). In a recent study, Feuchtner et al. (18) were able to demonstrate that the evaluation of rest myocardial CT-MPI in patients presenting with acute chest pain improved the accuracy of cardiac CT compared with SPECT, mainly by reducing the rate of false-positive findings. A recent study by Pursnani et al. (43) showed that early rest CT-MPI provided incremental value beyond obstructive CAD to detect acute coronary syndromes. Furthermore, coronary CTA plus rest CT-MPI was noninferior to coronary CTA plus SPECT (43).

One of the main shortcomings of CT-MPI is technical issues, such as beam hardening artifacts (BHA), which originate by the polychromatic nature of x-rays and the energy dependency of x-ray attenuation. These artifacts lead to a considerable myocardial signal density drop at regions adjacent to highly attenuated structures such as the sternum, spine, or descending aorta, thus resembling perfusion defects.

Dual-energy CT imaging has recently emerged as an appealing tool for CT-MPI given the ability of this technique to reduce BHA by the generation of synthesized monochromatic image reconstruction. There are currently 3 approaches to evaluate CT-MPI using dual-energy CT. The most widely used consists of a CT scanner equipped with 2 independent x-ray tubes and a set of detectors at an angular offset of 90° to 94° (depending on the generation), with 1 tube operating at 80 or 100 kV and the other operating at 140 kV (44,45). A second, more recent approach is based on a CT scanner with a single x-ray tube capable of ultrafast switching between 80 and 140 kV; therefore, it might have the potential to overcome some limitations of the former approach, such as increased

FIGURE 1 Myocardial Perfusion Imaging by CT

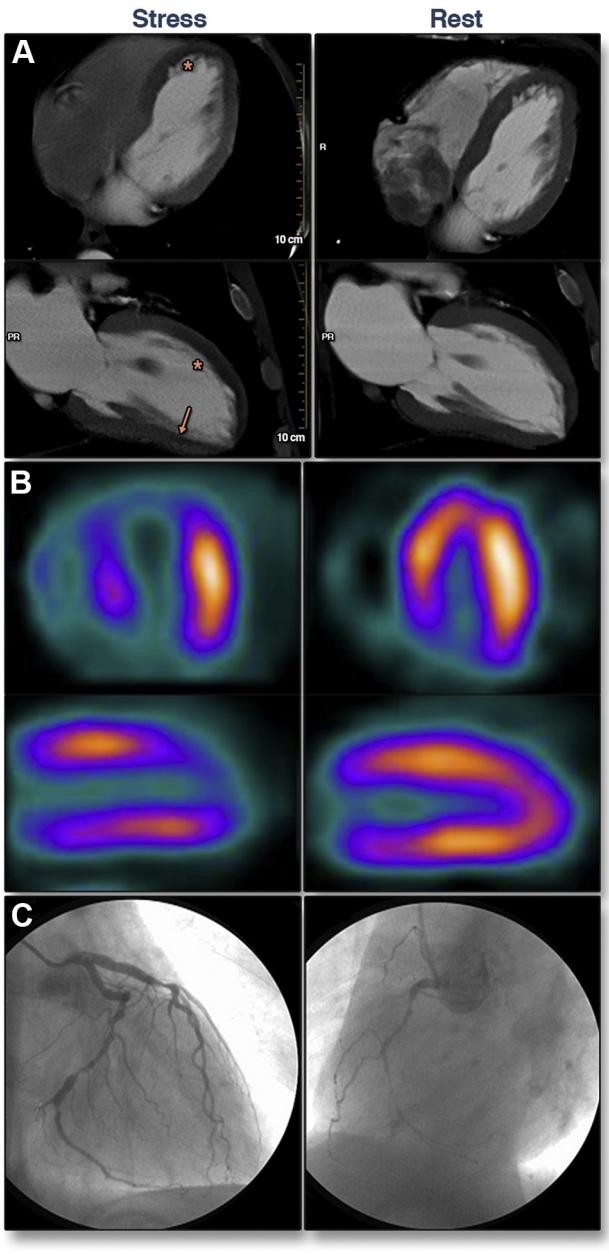

A 61-year-old man who was a previous smoker, had hypercholesterolemia, and had a body mass index of 32 kg/m^2. The patient had a history of established 3-vessel disease on previous invasive coronary angiography and currently had stable angina. Stress (dipyridamole) perfusion computed tomography (CT) **(A)** (mid-diastole 4- and 2-chamber multiplanar reconstruction (MPR) using a smooth filter are shown) was performed in view of the high pre-test coronary artery disease likelihood using conventional static CT-MPI protocol with a 256-detector scanner and demonstrated an extensive reversible perfusion defect at the anterior-wall **(*)** and a mild subendocardial reversible perfusion defect at the inferior wall **(arrow)**. Single photon emission CT confirmed the findings **(B)**. The patient was referred to invasive coronary angiography **(C)**, which showed 3-vessel disease with totally occluded right coronary artery, critical lesion at the left anterior descending artery, and severe lesion at the distal circumflex artery. MPI = myocardial perfusion imaging.

scattered radiation and potential mismatch in the projection views between high and low tube projections, when scanning moving objects such as the heart (46,47). A third approach is the dual-layer scanner consisting of 2 different scintillating materials fused together (sandwich). This application permits higher-energy x-ray photons to pass through the upper layer without having significant interaction, whereas the lower energy photons are mostly diminished in the top layer. The signals from the top and from the base constitute the 2 different energy ranges that have exactly the same projection (48). A number of studies have reported the incremental value of dual-energy stress CT-MPI over anatomic evaluation alone for the detection of reversible perfusion defects assessed by SPECT in patients with intermediate to high CAD likelihood (44,46,49). Moreover, another study showed improved diagnostic performance compared with conventional single-energy CT-MPI imaging, which was mainly attributed to the attenuation of BHA (50).

TRANSLUMINAL ATTENUATION GRADIENT AND CORRECTED CORONARY OPACIFICATION

Impairment of flow due to significant coronary stenosis is a phenomenon very well-studied with ICA, and its extent is assessed with Thrombolysis In Myocardial Infarction (TIMI) flow grades or corrected TIMI frame counts (51). Cardiac CT allows for the noninvasive assessment of coronary flow given the presence of isotemporal differences in contrast densities (i.e., contrast attenuation) between proximal and distal portions of the coronaries, especially evident in the presence of stenosis (52,53). For a given coronary cross section, the mean luminal contrast opacification in Hounsfield units (HU) is utilized, and several approaches have been described (54). Of note, contrast attenuation-based methods may be influenced by the time-density curve of the intravascular contrast agent and acquisition timing, as well as factors related to epicardial flow other than the presence of stenosis, which should be taken into account when assessing these measures (54,55). Unlike other functional tests that involve pharmacological stress, contrast attenuation is currently assessed only in a resting state.

TRANSLUMINAL ATTENUATION GRADIENT. Transluminal attenuation gradient (TAG) is the most studied attenuation-based method for the assessment of functional relevance of coronary stenosis (**Figure 2**). It involves the reconstruction of cross sections perpendicular to the centerline of the vessel at 5-mm intervals from the ostium to the distal level, where the vessel cross-sectional area falls below 2.0 mm^2. TAG is defined as the linear regression coefficient between luminal contrast attenuation (HU) and length from the ostium (cm) (53). The intended use of TAG is to better classify lesions in which the anatomic information is nonconclusive. Accordingly, lesion severity and plaque characteristics (i.e., calcified, noncalcified, or mixed) are integral components of the evaluation, especially because TAG has been shown to have a greater benefit in calcified lesions (56).

Current data are insufficient to recommend reference values for healthy arteries, and standard protocols for acquisition and interpretation may be needed (57). Steigner et al. (53) studied 108 healthy vessels from 36 patients using a 320-row multidetector computed tomography (MDCT) and showed that TAG was lowest in the right coronary artery (RCA) (-6.5 ± 4.1 HU/cm) and was similar for the left anterior descending artery and left circumflex artery (LCx) (-13.7 ± 8.0 HU/cm and -12.5 ± 7.8 HU/cm, respectively) (53). Cardiac phases correlated strongly with TAG values in the RCA and LCx, whereas heart rate showed a moderate correlation with those observed in the LCx.

Cutoff values for determining the functional relevance of coronary lesions have not been standardized and are diverse, as reflected in **Table 2** (55,56). Nonetheless, TAG decreases consistently and significantly with maximum stenosis severity on a per-vessel basis, especially in vessels with calcified lesions, as reported by Choi et al. (56) in a study including 370 coronaries from 126 patients using a 64-row MDCT scanner. Furthermore, the addition of TAG to the interpretation of coronary CTA may improve diagnostic accuracy, especially in the presence of calcified plaques (56,58).

Validation of TAG at rest for the determination of functionally significant stenosis using invasive FFR <0.8 as a reference has yielded conflicting results (59,60). Interestingly, in a study including 253 vessels from 85 patients evaluated with a 256-row MDCT, TAG did not provide incremental diagnostic accuracy over coronary CTA alone (61). However, after correction of temporal nonuniformity and exclusion of calcified coronary segments, a slight improvement in the net reclassification index was observed. Moreover, in a study assessing 127 vessels in 75 patients using a 320-row MDCT scanner, the investigators observed that in vessels without significant calcification or artifacts, TAG plus coronary CTA provided a comparable diagnostic accuracy when compared with coronary CTA combined with CT-MPI, although the sum of TAG + coronary CTA + CT-MPI offered the best diagnostic accuracy (61).

FIGURE 2 Representative Examples of TAG Measurements

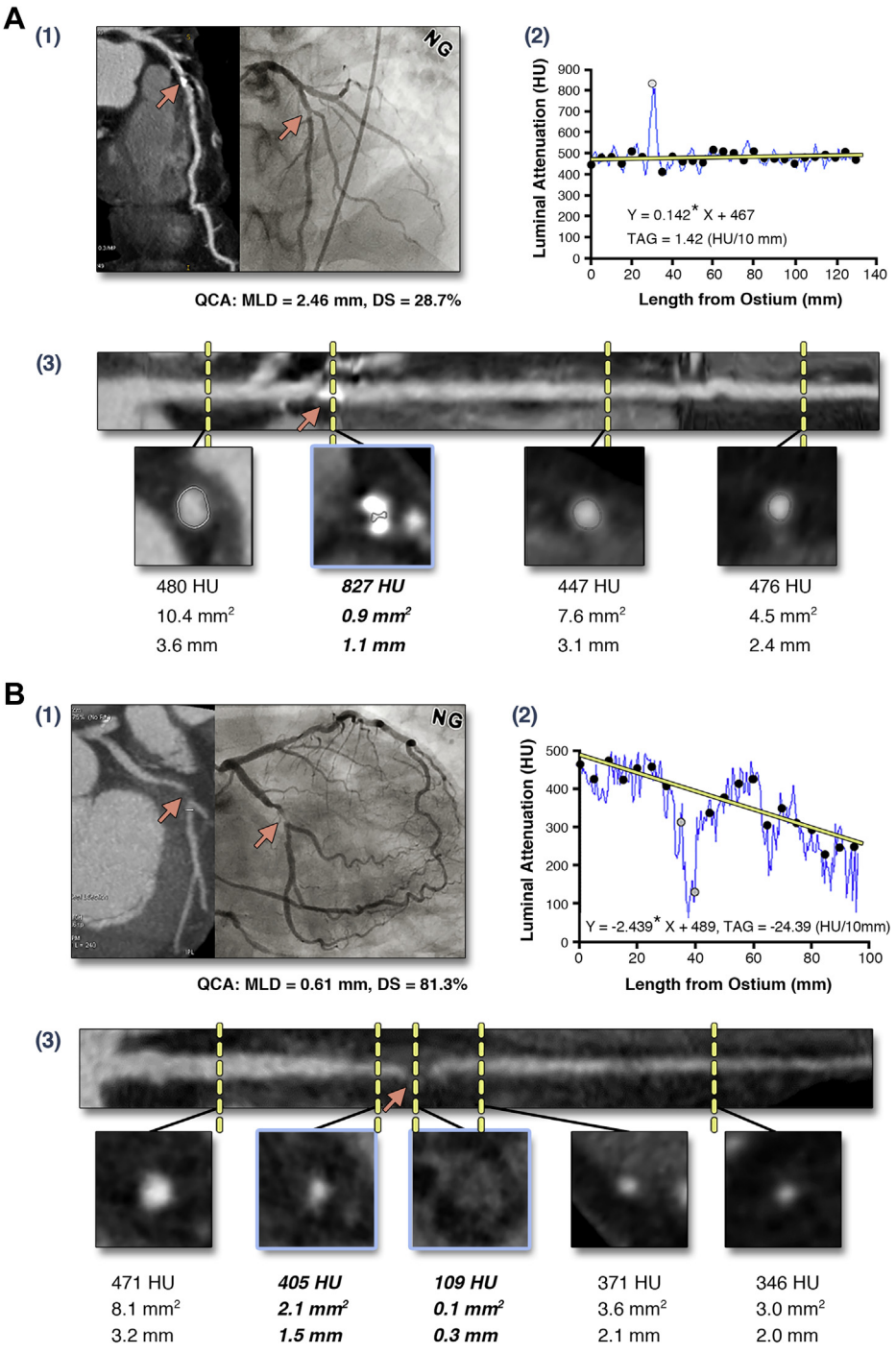

(A1) Calcified lesion in mid-left anterior descending artery that was indeterminate by coronary computed tomography angiography, but diameter stenosis was 28.7% by quantitative invasive coronary angiography. **Red arrows** correspond to stenotic sites. **(A2)** The intraluminal attenuation in distal left anterior descending artery does not decrease, demonstrating no significant obstruction. **(A3)** Cross-sectional views with **gray border** and sloped legend in **italics** represent excluded intervals. **(B)** Severe stenosis is shown in both coronary computed tomography angiography and invasive coronary angiography. It is confirmed in cross-sectional views. **Gray dots in A2 and B2** represent intervals that were excluded because of significant calcification or stenosis. Modified with permission from Choi et al. (56). DS = diameter stenosis; HU = Hounsfield units; MLD = minimum lumen diameter; NG = nitroglycerin; QCA = quantitative coronary angiography; TAG = transluminal attenuation gradient.

TABLE 1 Summarized Myocardial Perfusion Protocols

	Static Stress MPI	Dynamic Stress MPI
Scanner requirement	64-slice CT	Second-generation dual-source CT Wide detector CT with complete cardiac coverage
Acquisition mode	ECG-triggered axial scan mode ECG-gated spiral scan mode	ECG-triggered shuttle mode (dual-source CT) Stationary ECG-triggered mode (wide detector CT)
Contrast protocol	50–70 ml @ 4–5 ml/s	Short, high-rate bolus (≈50 ml)
Image data	Single high-resolution dataset	Sequence of low-resolution datasets
Effective dose	1–5 mSv*	5–10 mSv*
Output parameters	Attenuation values Relative attenuation values	Myocardial blood flow Myocardial blood volume

*Dose dependent on scanner technology and acquisition parameters.
CT = computed tomography; ECG = electrocardiogram; MPI = myocardial perfusion imaging.

CORRECTED CORONARY OPACIFICATION. CT scanners that are not capable of acquiring the whole heart in a single beat lack temporal uniformity for luminal contrast assessment. This temporal misalignment between subvolumes refers to differences in opacification induced by temporal changes between acquisitions of the superior versus inferior subvolumes. A proposed method to overcome this limitation is corrected contrast opacification (CCO), for which a quotient of the mean intraluminal HU in a coronary segment and the descending aorta in the same axial plane is calculated. CCO is assessed by the analysis of coronary CTA axial slices and calculates the quotient in the intracoronary segment most proximal and most distal to the stenosis. CCO is defined as the difference between these 2 quotients (59).

Although CCO has been shown to predict abnormal resting blood flow (TIMI flow grade <3, as determined with ICA) (62), its utility is still controversial because it does not improve diagnostic performance of CTA alone and available data are scarce (59). However, a combination of CCO with TAG has been proposed, yielding an improved discrimination of significant lesions compared with TAG alone (61). Of note, in a retrospective study including 106 patients treated with prior stenting, CCO was associated with in-stent restenosis severity in stents <3 mm in diameter (63).

FFR COMPUTED FROM CTA

Computational fluid dynamics (CFD), as applied to cardiac CT images, is a novel method that enables prediction of blood flow and pressure fields in coronary arteries and calculation of lesion-specific FFR (64–66). The FFR is computed from commonly acquired MDCT scans (FFR_{CT}) without any modification of cardiac CT protocols, additional image acquisition, or administration of medications.

The FFR_{CT} technology is based on 3 key principles. The first is that coronary supply meets myocardial demand at rest (total resting coronary flow is relative to ventricular mass). The second is that resistance of the microcirculation at rest is inversely but not linearly proportional to the size of the feeding vessel. The third principle is that microcirculation reacts predictably to maximal hyperemic conditions in patients with normal coronary flow. On the basis of these principles, a lumped parameter model representing the resistance to flow during simulated hyperemia is applied to each coronary branch of the segmented coronary CTA model. The FFR_{CT} was modeled for

TABLE 2 Studies Evaluating TAG for the Identification of Ischemic Lesions

Year	First Author (Ref. #)	CT Generation	No. of Vessels (n)	Calcified Lesions (%)	Reference	Improved Diagnostic Accuracy	Cutoffs and Components	Se	Sp	PPV	NPV	Significant NRI
2011	Choi et al. (56)	64	370 (126)	27	CAG ≥50%	Yes	≤−1.80 HU/cm + DS ≥50%	84	94	96	75	Yes
2012	Choi et al. (59)	64	97 (63)	32	FFR <0.80	Yes	≤−0.654 HU/mm + DS ≥50%	90	63	63	90	No
2012	Yoon et al. (60)	64	82 (53)	29	FFR ≤0.80	NA	≤−0.654 HU/mm	38	88	67	69	NA
2013	Wong et al. (55)	320	78 (54)	69	FFR ≤0.80	Yes	≤−15.1 HU/cm	77	74	67	83	Yes
2014	Zheng et al. (58)	64	309 (107)	37	CAG ≥50%	Yes	≤−11.33 HU/cm + DS ≥50%	94	94	90	96	No
2014	Wong et al. (79)	320	97 (75)	39	FFR ≤0.80	Yes	≤−15.1 HU/cm + DS ≥50%	73	97	92	87	Yes
2014	Stuijfzand et al. (61)	256	225 (85)	34	FFR ≤0.80	No	≤−7.51 HU/cm	69	44	83	27	No
2015	Hell et al. (80)	Dual-source	72 (59)	NA	FFR ≤0.80	No	≤−0.65 HU/mm	57	61	28	31	NA
2015	Wang et al. (81)	Dual-source	32 (32)	NA	FFR <0.80	No	≤−1.51 HU/mm	37	58	23	73	NA

CAG = coronary angiography; DS = diameter stenosis; FFR = fractional flow reserve; HU = Hounsfield units; NA = not available; NPV = negative predictive value; NRI = net reclassification improvement; PPV = positive predictive value; Se = sensitivity; Sp = specificity; TAG = transluminal attenuation gradient.

FIGURE 3 Fractional Flow Reserve CT

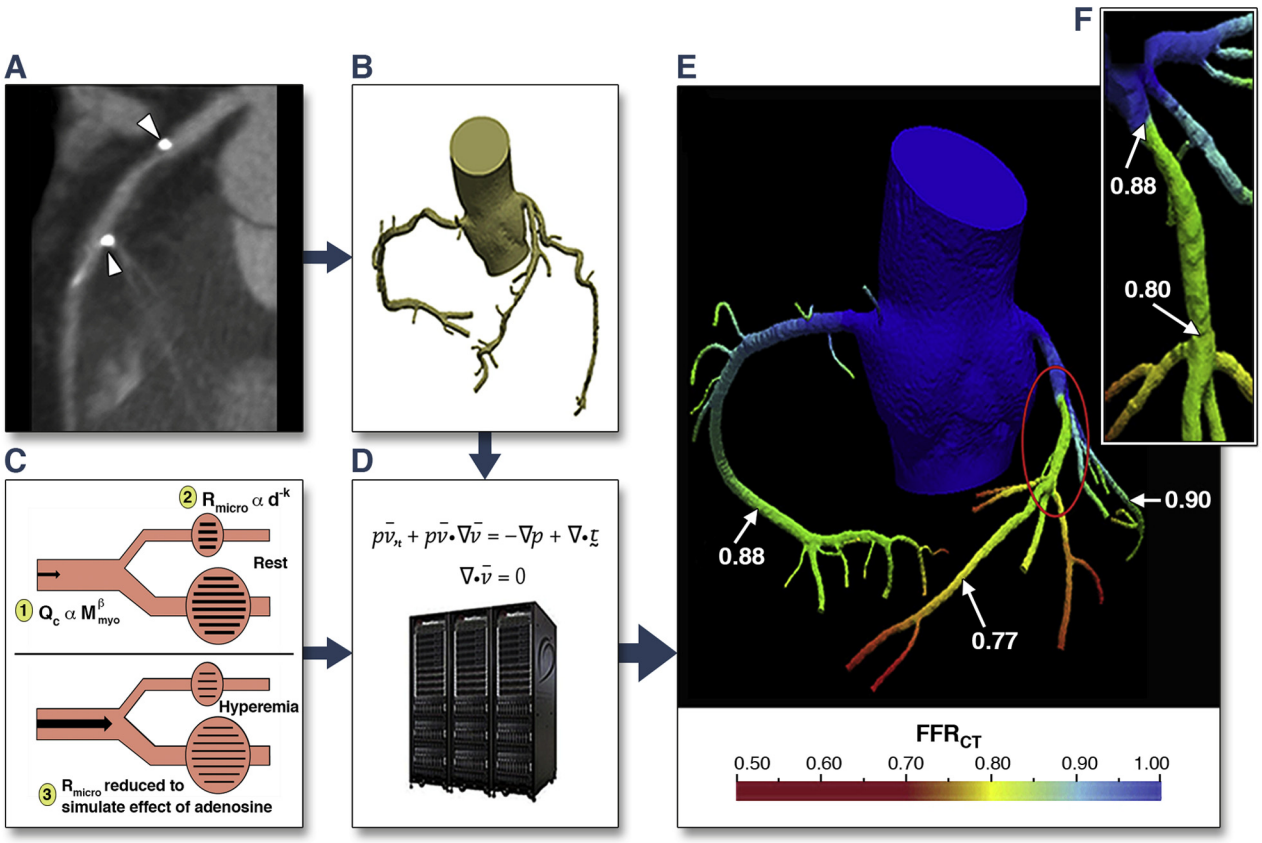

Standard coronary computed tomography angiography data are obtained. **(A)** The 5-year results following an Absorb implantation are shown. **Arrowheads** indicate the 2 metallic markers in the left anterior descending artery. Noncalcified plaque results in 62% area stenosis. **(B)** A quantitative 3-dimensional anatomic model is generated. **(C)** A physiological model of the coronary microcirculation is derived from patient-specific data with 3 main principles: 1) resting coronary flow proportional to myocardial mass; 2) microvascular resistance inversely proportional to vessel size; and 3) microvascular resistance reduced to simulate maximal hyperemia. **(D)** Physical laws of fluid dynamics are applied to compute coronary blood flow. **(E)** Fractional flow reserve computed tomography (FFR_{CT}) is calculated throughout the coronary arteries. **(F)** From the proximal to the distal edge of the scaffold, the FFR_{CT} decreases from 0.88 to 0.80. Modified with permission from Garcia-Garcia et al. (78).

conditions of adenosine-induced hyperemia; an FFR_{CT} ≤0.80 was considered to be diagnostic of lesion-specific ischemia (67) (**Figure 3**).

The most advanced FFR_{CT} is from HeartFlow (Redwood City, California), and at present, there have been 3 studies (67-69) using this technology (**Table 3**). In all studies, FFR_{CT} has been shown to be superior to conventional cardiac CT and had good predictive accuracies when compared with invasive FFR. However, this technology requires processing on a powerful remote computer for off-line analysis. The adjustments of computational CT-based FFR algorithm by reduced-order algorithm without the need for data transfer have been developed to provide patient management guidance within clinically viable time frames (processing time <1 h). The feasibility of this approach has been tested by 2 retrospective studies using a software research prototype (Siemens cFFR, version 1.4, Siemens Healthcare, Malvern, Pennsylvania; currently not commercially available) (70,71). With this technique, the mean total time for processing and flow computation was 51.9 ± 9.0 min/study, and there was a good direct correlation between CT-based FFR and invasively derived FFR (Pearson's product-moment $r = 0.74$; $p < 0.0001$). The validity of an on-site algorithm compared with that of coronary CTA has been reported with an accuracy for cFFR (area under the curve 0.83) over coronary CTA alone (area under the curve 0.64).

Besides the dependence on a remote evaluation (with time-delay and additional cost issues), FFR_{CT} is associated with 2 other limitations. The first is

TABLE 3 Trials Comparing FFR-$_{CT}$ (HeartFlow) and Invasive FFR

	DISCOVER-FLOW (67)	DeFACTO (68)	NXT (69)
Publication year	2011	2012	2014
Patients profile, n	Stable CAD, 103	Stable CAD, 252	Stable CAD, 254
Coronary CTA ≥50%–AUC	0.61	0.64	0.53
Coronary CTA ≥50%			
Specificity	25%	42%	34%
Sensitivity	94%	84%	94%
PPV	58%	61%	40%
NPV	80%	72%	92%
FFR_{CT} ≤0.80			
AUC	0.87	0.73	0.81
Specificity	82%	54%	79%
Sensitivity	93%	90%	86%
PPV	85%	67%	65%
NPV	91%	84%	93%
Prevalence of FFR ≤0.80	56%	54%	42%
% patients excluded due to nonevaluable scans	NA	12%	13%
CT generation	≥64 detector row	≥64 detector row	≥64 detector row
Primary CT reading	Core laboratory	Core laboratory	Local investigator
Software version	NA	1.2	1.4

AUC, specificity, sensitivity, PPV, and NPV are for per-patient analysis.

AUC = area under the curve; CT = computed tomography; CTA = computed tomographic angiography; DeFACTO = Determination of Fractional Flow Reserve by Anatomic Computed Tomographic Angiography; DISCOVER-FLOW = Diagnosis of Ischemia-Causing Stenoses Obtained Via Noninvasive Fractional Flow Reserve; FFR = fractional flow reserve; NPV = negative predictive value; NXT = Analysis of Coronary Blood Flow Using CT Angiography: Next Steps; PPV = positive predictive value.

the dependence on very high image quality. In the published studies performed in experienced cardiac CT centers, even after excluding patients with high body mass index, atrial fibrillation, and previous percutaneous coronary intervention or coronary artery bypass graft, a significant percentage of patients (up to 13%) were not evaluable due to insufficient image quality (**Table 3**). The other limitation is that information about plaque burden is not considered for the calculations, and recently, the relation between atherosclerotic plaque features identified by coronary CTA and the presence of ischemia has been underlined (9,72).

EXTRAPOLATION FROM ATHEROSCLEROTIC PLAQUE CHARACTERISTICS

Recently, the issue of whether functional information can be extracted from the anatomic-based information obtained with cardiac CT has been explored further. In a study by Park et al. (72), the authors were able to document an association between certain atherosclerotic plaque characteristics (APCs), depicted by coronary CTA (**Figure 4**, **Table 4**) and the presence of ischemia by invasive FFR (72). In this study, 252 stable patients without a previous revascularization procedure were included and simultaneously evaluated by coronary CTA and ICA, with FFR as gold standard for functional significance. Among the cardiac CT obstructive (≥50% stenosis) lesions, the authors found that only one-half of them were functionally significant by FFR, and the independent predictors of ischemia were lesion length, positive remodeling (index ≥1.1), and the presence of low attenuation plaque (<30 HU). The presence of 2 or more of these APCs was associated with a 13-fold increased odds of ischemia by invasive FFR, and spotty calcification, another APC evaluated, was not an independent predictor of ischemia. In another study including 58 patients with intermediate stenosis on coronary CTA undergoing ICA with FFR, aggregate plaque volume, reflecting the extent of coronary atherosclerotic burden, was incremental to several luminal narrowing measurements (diameter stenosis, area stenosis, minimum luminal diameter, minimum lumen area) to predict functional significance (FFR <0.80) (9). In another small study evaluating 42 patients with similar methodology, coronary CTA measurements of area stenosis and lesion length were the strongest determinants of an abnormal FFR (73).

The discordance between ischemia and stenosis has been pointed out in several FFR studies. In a recent prospective cohort of 1,000 patients evaluated simultaneously by ICA, IVUS, and FFR, up to 57% of the lesions with stenosis ≥50% had an FFR >0.80, and conversely and more interesting, 16% of the nonobstructive lesions were reversed mismatches, because they were associated with FFR<0.80 (74). In the coronary CTA study from Park et al. (72), the authors also found a 17% rate of ischemia among nonobstructive (<50% stenosis) lesions, which is remarkable. The percentage of patients considered as anatomy-function mismatches has to be interpreted in view of the threshold for significant stenosis, and a 50% stenosis cutoff is not very ambitious and easily leads to a significant subgroup of false-positive patients (without ischemia, despite the presence of a "significant" stenosis). In this regard, their counterparts might be considered as "false negative" (with ischemia, but without a significant stenosis), and this subgroup of patients might explain the worse than expected prognosis of patients with nonobstructive CAD but high disease burden, which has been extensively documented with calcium scoring (75) and has also been recently demonstrated with the use of coronary atherosclerotic burden scores (76,77). Bittencourt et al. (76) evaluated 3,242 patients without known CAD referred for coronary CTA and followed up for a median of 3.6 years and demonstrated that disease extent (as assessed by the number of segments with extensive disease [defined as ≥5 segments

FIGURE 4 Extrapolation From Atherosclerotic Plaque Characteristics

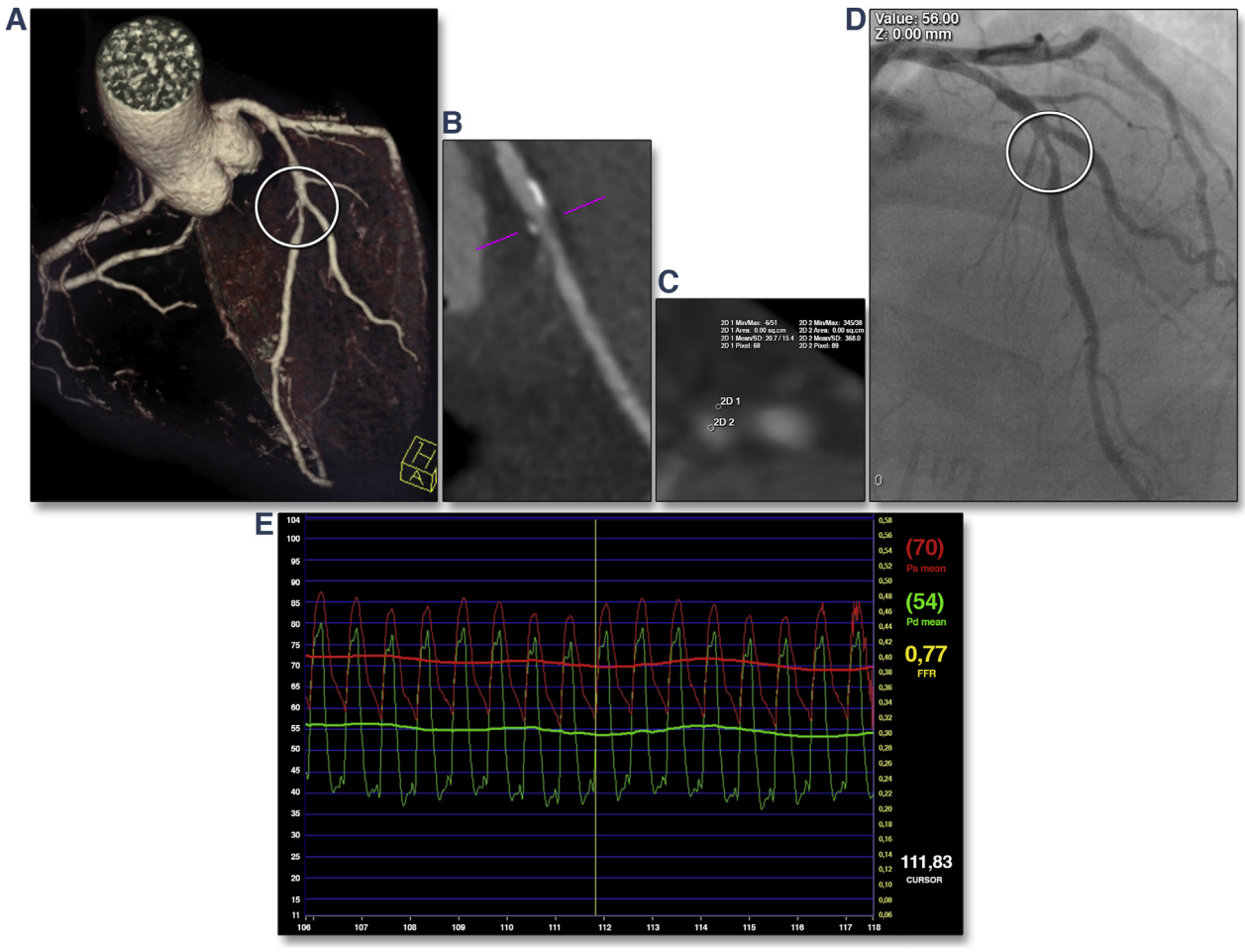

In the **left panels** (**A**: volume-rendering technique; **B and C**: multiplanar reconstructions), coronary computed tomography angiography depicting a mixed plaque in the mid-segment of the left anterior descending artery (LAD) with intermediate stenosis (50% to 70%) and several features that have been associated with the presence of ischemia and/or future events: spotty calcification **(A and B)**, positive remodeling **(B and C)**, and low attenuation plaque **(C)**. In the **right panels**, the corresponding invasive coronary angiography image **(D)** and the result of the fractional flow reserve (FFR), which was in the gray zone: 0.77 **(E)**. The **pink line** in **B** represents the region depicted by the cross sectional image in **C**. The final clinical judgment was to proceed to revascularization, and the patient was submitted to percutaneous coronary intervention. Pa = aortic pressure; Pd = distal coronary pressure across the stenosis.

with CAD]) has independent and incremental prognostic value for predicting cardiovascular death and myocardial infarction. In another recent study, Mushtaq et al. (77), using a more comprehensive CAD burden index—the CT-Leaman score (CT-LeSc) with information on lesion location, stenosis, and plaque composition—evaluated the prognostic effect of atherosclerotic burden among 1,304 patients undergoing coronary CTA for suspected CAD and followed up for a mean of 52 months (77). The authors found that event-free survival in nonobstructive (<50% stenosis) CAD but high (>5) CT-LeSc was similar to

TABLE 4 Coronary CTA Plaque Characteristics Associated With Ischemia

Plaque Features	Cutoff	Independent Predictor of Ischemia	Ref. #
Area stenosis	Per 5%	Yes	(72,73)
Lesion length	Per mm	Yes	(72,73)
Positive remodeling	>1.1	Yes	(72)
Low attenuation plaque	<30 HU	Yes	(72)
Spotty calcification	<3 mm	No	(72)
Aggregate plaque volume, %	per 5%	Yes	(9,72)

CTA = computed tomographic angiography; HU = Hounsfield units.

JACC: CARDIOVASCULAR IMAGING, VOL. 8, NO. 11, 2015
NOVEMBER 2015:1322–35

CENTRAL ILLUSTRATION **Functional Evaluation by Cardiac CT**

MYOCARDIAL PERFUSION IMAGING

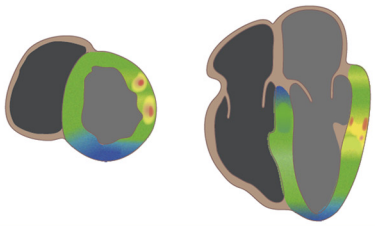

Main Features:

- Static Stress MPI: single high-resolution CT angiogram during pharmacological vasodilation for semi-quantitative analyses
- Dynamic Stress MPI: sequence of low-resolution datasets to calculate the absolute myocardial blood flow from time-attenuation curves

Current Limitations:

- Additional contrast medium, pharmacological stress and radiation
- Beam hardening artifacts
- Dynamic MPI requires wide detector coverage and shuttle mode acquisition
- Limited experience and validation, and requires more radiation

CORONARY ATTENUATION PATTERNS

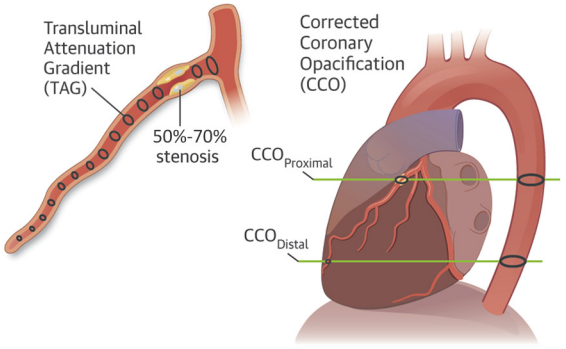

Main Features:

- TAG: linear regression coefficient between luminal contrast attenuation (HU) and length from the ostium
- CCO: contrast opacification corrected for the descending aorta in the same axial plane

Current Limitations:

- Lack of standardized cut-off values for functional significance
- Limited data and some conflicting results

CTA DERIVED FRACTIONAL FLOW RESERVE

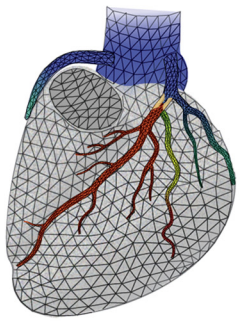

Main Features:

- Computed using computational fluid dynamics from regular CT angiograms without protocol modification or additional medication
- Improved diagnostic accuracy vs CTA alone, mainly due to higher specificity

Current Limitations:

- Remote evaluation
- Dependence on high image quality

ATHEROSCLEROTIC PLAQUE CHARACTERISTICS

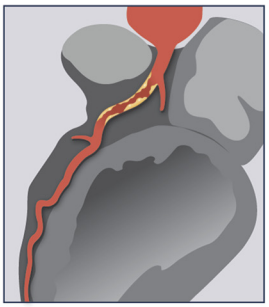

Main Features:

- Lesion length, low attenuation plaque, positive remodeling, and aggregate plaque volume associated with ischemia by invasive FFR

Current Limitations:

- Dependence on high image quality
- Spatial resolution
- Low attenuation plaque cut-off influenced by several factors

de Araújo Gonçalves, P. et al. J Am Coll Cardiol Img. 2015; 8(11):1322–35.

This illustration depicts the main features and current limitations of 4 different lines developed in the search for functional information with cardiac CT. CCO = corrected coronary opacification; CT = computed tomography; FFR = fractional flow reserve; MPI = myocardial perfusion imaging; TAG = transluminal attenuation gradients.

obstructive CAD with high CT-LeSc but lower than obstructive CAD with low CT-LeSc. These 2 studies reinforce the concept that disease burden (either >5 segments with disease or a CT-LeSc >5) is an independent long-term predictor of hard cardiac events beyond stenosis severity and is in line with the results of the studies linking APCs (72) and aggregate plaque volume (9) with the presence of ischemia even among (apparently) nonobstructive CAD lesions.

CONCLUSIONS

The discordance between ischemia and stenosis that has been pointed out in several ICA and coronary CTA studies and the central role that ischemia plays in clinical decision making are both the main drivers in the search for functional information in cardiac CT. Several different lines have been reviewed in the present paper, as shown in the **Central Illustration**, and although some of these areas require additional software and hardware refinements so that they can have a more robust performance, the impressive development of cardiac CT in recent years and its wide clinical adoption leads us to believe that functional evaluation of CAD by cardiac CT will certainly move from research to a routine clinical tool in a near future.

Certain atherosclerotic plaque features, depicted by coronary CTA, have recently emerged as possibly related to the presence of ischemia and, more importantly, might help to predict the future risk of cardiovascular events.

REPRINT REQUESTS AND CORRESPONDENCE: Dr. Hector M. Garcia-Garcia, Thoraxcenter-Erasmus Medical Center, z120 Dr Molerwaterplein 40, 3015 GD Rotterdam, the Netherlands. E-mail: hect2701@gmail.com.

REFERENCES

1. Budoff MJ, Dowe D, Jollis JG, et al. Diagnostic performance of 64-multidetector row coronary computed tomographic angiography for evaluation of coronary artery stenosis in individuals without known coronary artery disease: results from the prospective multicenter ACCURACY (Assessment by Coronary Computed Tomographic Angiography of Individuals Undergoing Invasive Coronary Angiography) trial. J Am Coll Cardiol 2008;52:1724–32.

2. Meijboom WB, Meijs MF, Schuijf JD, et al. Diagnostic accuracy of 64-slice computed tomography coronary angiography: a prospective, multicenter, multivendor study. J Am Coll Cardiol 2008;52:2135–44.

3. Pijls NH, van Schaardenburgh P, Manoharan G, et al. Percutaneous coronary intervention of functionally nonsignificant stenosis: 5-year follow-up of the DEFER study. J Am Coll Cardiol 2007;49:2105–11.

4. Tonino PA, De Bruyne B, Pijls NH, et al. Fractional flow reserve versus angiography for guiding percutaneous coronary intervention. N Engl J Med 2009;360:213–24.

5. Shaw LJ, Berman DS, Maron DJ, et al. Optimal medical therapy with or without percutaneous coronary intervention to reduce ischemic burden: results from the Clinical Outcomes Utilizing Revascularization and Aggressive Drug Evaluation (COURAGE) trial nuclear substudy. Circulation 2008;117:1283–91.

6. Montalescot G, Sechtem U, Achenbach S, et al., for the Task Force Members. 2013 ESC guidelines on the management of stable coronary artery disease: the Task Force on the Management of Stable Coronary Artery Disease of the European Society of Cardiology. Eur Heart J 2013;34:2949–3003.

7. Meijboom WB, van Mieghem CA, Mollet NR, et al. 64-slice computed tomography coronary angiography in patients with high, intermediate, or low pretest probability of significant coronary artery disease. J Am Coll Cardiol 2007;50:1469–75.

8. Vavere AL, Arbab-Zadeh A, Rochitte CE, et al. Coronary artery stenoses: accuracy of 64-detector row CT angiography in segments with mild, moderate, or severe calcification—a subanalysis of the CORE-64 trial. Radiology 2011;261:100–8.

9. Nakazato R, Shalev A, Doh JH, et al. Aggregate plaque volume by coronary computed tomography angiography is superior and incremental to luminal narrowing for diagnosis of ischemic lesions of intermediate stenosis severity. J Am Coll Cardiol 2013;62:460–7.

10. Naya M, Murthy VL, Blankstein R, et al. Quantitative relationship between the extent and morphology of coronary atherosclerotic plaque and downstream myocardial perfusion. J Am Coll Cardiol 2011;58:1807–16.

11. Mancini GB, Hartigan PM, Shaw LJ, et al. Predicting outcome in the COURAGE trial (Clinical Outcomes Utilizing Revascularization and Aggressive Drug Evaluation): coronary anatomy versus ischemia. J Am Coll Cardiol Intv 2014;7:195–201.

12. Panza JA, Holly TA, Asch FM, et al. Inducible myocardial ischemia and outcomes in patients with coronary artery disease and left ventricular dysfunction. J Am Coll Cardiol 2013;61:1860–70.

13. George RT, Arbab-Zadeh A, Miller JM, et al. Computed tomography myocardial perfusion imaging with 320-row detector computed tomography accurately detects myocardial ischemia in patients with obstructive coronary artery disease. Circ Cardiovasc Imaging 2012;5:333–40.

14. Bettencourt N, Rocha J, Ferreira N, et al. Incremental value of an integrated adenosine stress-rest MDCT perfusion protocol for detection of obstructive coronary artery disease. J Cardiovasc Comput Tomogr 2011;5:392–405.

15. Magalhaes TA, Cury RC, Pereira AC, et al. Additional value of dipyridamole stress myocardial perfusion by 64-row computed tomography in patients with coronary stents. J Cardiovasc Comput Tomogr 2011;5:449–58.

16. Bischoff B, Bamberg F, Marcus R, et al. Optimal timing for first-pass stress CT myocardial perfusion imaging. Int J Cardiovasc Imaging 2013;29:435–42.

17. Ko SM, Choi JW, Hwang HK, Song MG, Shin JK, Chee HK. Diagnostic performance of combined noninvasive anatomic and functional assessment with dual-source CT and adenosine-induced stress dual-energy CT for detection of significant coronary stenosis. AJR Am J Roentgenol 2012;198:512–20.

18. Feuchtner GM, Plank F, Pena C, et al. Evaluation of myocardial CT perfusion in patients presenting with acute chest pain to the emergency department: comparison with SPECT-myocardial perfusion imaging. Heart 2012;98:1510–7.

19. Bamberg F, Marcus RP, Becker A, et al. Dynamic myocardial CT perfusion imaging for evaluation of myocardial ischemia as determined by MR imaging. J Am Coll Cardiol Img 2014;7:267–77.

20. George RT, Jerosch-Herold M, Silva C, et al. Quantification of myocardial perfusion using dynamic 64-detector computed tomography. Invest Radiol 2007;42:815–22.

21. Rossi A, Dharampal A, Wragg A, et al. Diagnostic performance of hyperaemic myocardial blood flow index obtained by dynamic computed tomography: does it predict functionally significant coronary lesions? Eur Heart J Cardiovasc Imaging 2014;15:85–94.

22. Rossi A, Uitterdijk A, Dijkshoorn M, et al. Quantification of myocardial blood flow by adenosine-stress CT perfusion imaging in pigs during various degrees of stenosis correlates well with coronary artery blood flow and fractional

flow reserve. Eur Heart J Cardiovasc Imaging 2013; 14:331–8.

23. Bamberg F, Hinkel R, Schwarz F, et al. Accuracy of dynamic computed tomography adenosine stress myocardial perfusion imaging in estimating myocardial blood flow at various degrees of coronary artery stenosis using a porcine animal model. Invest Radiol 2012;47:71–7.

24. So A, Wisenberg G, Islam A, et al. Non-invasive assessment of functionally relevant coronary artery stenoses with quantitative CT perfusion: preliminary clinical experiences. Eur Radiol 2012; 22:39–50.

25. Greif M, von Ziegler F, Bamberg F, et al. CT stress perfusion imaging for detection of haemodynamically relevant coronary stenosis as defined by FFR. Heart 2013;99:1004–11.

26. Bamberg F, Becker A, Schwarz F, et al. Detection of hemodynamically significant coronary artery stenosis: incremental diagnostic value of dynamic CT-based myocardial perfusion imaging. Radiology 2011;260:689–98.

27. Mahnken AH, Klotz E, Pietsch H, et al. Quantitative whole heart stress perfusion CT imaging as noninvasive assessment of hemodynamics in coronary artery stenosis: preliminary animal experience. Invest Radiol 2010;45:298–305.

28. Rossi A, Merkus D, Klotz E, Mollet N, de Feyter PJ, Krestin GP. Stress myocardial perfusion: imaging with multidetector CT. Radiology 2014; 270:25–46.

29. Ho KT, Chua KC, Klotz E, Panknin C. Stress and rest dynamic myocardial perfusion imaging by evaluation of complete time-attenuation curves with dual-source CT. J Am Coll Cardiol Img 2010; 3:811–20.

30. Feuchtner G, Goetti R, Plass A, et al. Adenosine stress high-pitch 128-slice dual-source myocardial computed tomography perfusion for imaging of reversible myocardial ischemia: comparison with magnetic resonance imaging. Circ Cardiovasc Imaging 2011;4:540–9.

31. Kurata A, Kawaguchi N, Kido T, et al. Qualitative and quantitative assessment of adenosine triphosphate stress whole-heart dynamic myocardial perfusion imaging using 256-slice computed tomography. PloS one 2013;8:e83950.

32. Ko BS, Cameron JD, Meredith IT, et al. Computed tomography stress myocardial perfusion imaging in patients considered for revascularization: a comparison with fractional flow reserve. Eur Heart J 2012;33:67–77.

33. Bastarrika G, Ramos-Duran L, Rosenblum MA, Kang DK, Rowe GW, Schoepf UJ. Adenosine-stress dynamic myocardial CT perfusion imaging: initial clinical experience. Invest Radiol 2010;45: 306–13.

34. George RT, Mehra VC, Chen MY, et al. Myocardial CT perfusion imaging and SPECT for the diagnosis of coronary artery disease: a head-to-head comparison from the CORE320 multicenter diagnostic performance study. Radiology 2014;272:407–16.

35. Cury RC, Kitt TM, Feaheny K, et al. A randomized, multicenter, multivendor study of myocardial perfusion imaging with regadenoson CT perfusion vs single photon emission CT. J Cardiovasc Comput Tomogr 2015;9:103–12. e1–2.

36. Rodriguez-Granillo GA, Rosales MA, Baum S, et al. Early assessment of myocardial viability by the use of delayed enhancement computed tomography after primary percutaneous coronary intervention. J Am Coll Cardiol Img 2009;2: 1072–81.

37. Sato A, Nozato T, Hikita H, et al. Prognostic value of myocardial contrast delayed enhancement with 64-slice multidetector computed tomography after acute myocardial infarction. J Am Coll Cardiol 2012;59:730–8.

38. Schuleri KH, Centola M, George RT, et al. Characterization of peri-infarct zone heterogeneity by contrast-enhanced multidetector computed tomography: a comparison with magnetic resonance imaging. J Am Coll Cardiol 2009;53: 1699–707.

39. Nieman K, Shapiro MD, Ferencik M, et al. Reperfused myocardial infarction: contrast-enhanced 64-Section CT in comparison to MR imaging. Radiology 2008;247:49–56.

40. Carrascosa P, Deviggiano A, Capunay C, De Zan MC, Goldsmit A, Rodriguez-Granillo GA. Effect of intracycle motion correction algorithm on image quality and diagnostic performance of computed tomography coronary angiography in patients with suspected coronary artery disease. Acad Radiol 2015;22:81–6.

41. de Araújo Gonçalves P, Jerónimo Sousa P, Calé R, et al. Radiation effective dose of three diagnostic tests in cardiology: single-photon emission computed tomography, invasive coronary angiography and cardiac computed tomography angiography. Rev Port Cardiol 2013;32:981–6.

42. Ichinose T, Yamase M, Yokomatsu Y, et al. Acute myocardial infarction with myocardial perfusion defect detected by contrast-enhanced computed tomography. Intern Med 2009;48: 1235–8.

43. Pursnani A, Lee AM, Mayrhofer T, et al. Early resting myocardial computed tomography perfusion for the detection of acute coronary syndrome in patients with coronary artery disease. Circ Cardiovasc Imaging 2015;8:e002404.

44. Weininger M, Schoepf UJ, Ramachandra A, et al. Adenosine-stress dynamic real-time myocardial perfusion CT and adenosine-stress first-pass dual-energy myocardial perfusion CT for the assessment of acute chest pain: initial results. Eur J Radiol 2012;81:3703–10.

45. Ko SM, Choi JW, Song MG, et al. Myocardial perfusion imaging using adenosine-induced stress dual-energy computed tomography of the heart: comparison with cardiac magnetic resonance imaging and conventional coronary angiography. Eur Radiol 2011;21:26–35.

46. Carrascosa PM, Deviggiano A, Capunay C, et al. Incremental value of myocardial perfusion over coronary angiography by spectral computed tomography in patients with intermediate to high likelihood of coronary artery disease. Eur J Radiol 2015;84:637–42.

47. Rodriguez-Granillo GA, Carrascosa P, Cipriano S, et al. Beam hardening artifact reduction using dual energy computed tomography: implications for myocardial perfusion studies. Cardiovasc Diagn Ther 2015;5:79–85.

48. Boll DT, Merkle EM, Paulson EK, Fleiter TR. Coronary stent patency: dual-energy multidetector CT assessment in a pilot study with anthropomorphic phantom. Radiology 2008;247: 687–95.

49. Ruzsics B, Lee H, Zwerner PL, Gebregziabher M, Costello P, Schoepf UJ. Dual-energy CT of the heart for diagnosing coronary artery stenosis and myocardial ischemia-initial experience. Eur Radiol 2008;18:2414–24.

50. Carrascosa PM, Cury RC, Deviggiano A, et al. Comparison of myocardial perfusion evaluation with single versus dual-energy CT and effect of beam-hardening artifacts. Acad Radiol 2015;22: 591–9.

51. Gibson CM, Cannon CP, Daley WL, et al. TIMI frame count: a quantitative method of assessing coronary artery flow. Circulation 1996; 93:879–88.

52. Rybicki FJ, Otero HJ, Steigner ML, et al. Initial evaluation of coronary images from 320-detector row computed tomography. Int J Cardiovasc Imaging 2008;24:535–46.

53. Steigner ML, Mitsouras D, Whitmore AG, et al. Iodinated contrast opacification gradients in normal coronary arteries imaged with prospectively ECG-gated single heart beat 320-detector row computed tomography. Circ Cardiovasc Imaging 2010;3:179–86.

54. Loewe C, Stadler A. Computed tomography assessment of hemodynamic significance of coronary artery disease: CT perfusion, contrast gradients by coronary CTA, and fractional flow reserve review. J Thorac Imaging 2014;29:163–72.

55. Wong DT, Ko BS, Cameron JD, et al. Transluminal attenuation gradient in coronary computed tomography angiography is a novel noninvasive approach to the identification of functionally significant coronary artery stenosis: a comparison with fractional flow reserve. J Am Coll Cardiol 2013;61: 1271–9.

56. Choi JH, Min JK, Labounty TM, et al. Intracoronary transluminal attenuation gradient in coronary CT angiography for determining coronary artery stenosis. J Am Coll Cardiol Img 2011;4: 1149–57.

57. Chatzizisis YS, George E, Cai T, et al. Accuracy and reproducibility of automated, standardized coronary transluminal attenuation gradient measurements. Int J Cardiovasc Imaging 2014;30: 1181–9.

58. Zheng M, Wei M, Wen D, et al. Transluminal attenuation gradient in coronary computed tomography angiography for determining stenosis severity of calcified coronary artery: a primary study with dual-source CT. Eur Radiol 2015;25: 1219–28.

59. Choi JH, Koo BK, Yoon YE, et al. Diagnostic performance of intracoronary gradient-based methods by coronary computed tomography angiography for the evaluation of physiologically significant coronary artery stenoses: a validation study with fractional flow reserve. Eur Heart J Cardiovasc Imaging 2012;13:1001–7.

60. Yoon YE, Choi JH, Kim JH, et al. Noninvasive diagnosis of ischemia-causing coronary stenosis using CT angiography: diagnostic value of transluminal attenuation gradient and fractional flow reserve computed from coronary CT angiography compared to invasively measured fractional flow reserve. J Am Coll Cardiol Img 2012;5:1088–96.

61. Stuijfzand WJ, Danad I, Raijmakers PG, et al. Additional value of transluminal attenuation gradient in CT angiography to predict hemodynamic significance of coronary artery stenosis. J Am Coll Cardiol Img 2014;7:374–86.

62. Chow BJ, Kass M, Gagne O, et al. Can differences in corrected coronary opacification measured with computed tomography predict resting coronary artery flow? J Am Coll Cardiol 2011;57:1280–8.

63. Gao Y, Lu B, Hou ZH, et al. Coronary in-stent restenosis: assessment with corrected coronary opacification difference across coronary stents measured with CT angiography. Radiology 2015; 275:403–12.

64. Kim HJ, Jansen KE, Taylor CA. Incorporating autoregulatory mechanisms of the cardiovascular system in three-dimensional finite element models of arterial blood flow. Ann Biomed Eng 2010;38: 2314–30.

65. Kim HJ, Vignon-Clementel IE, Coogan JS, Figueroa CA, Jansen KE, Taylor CA. Patient-specific modeling of blood flow and pressure in human coronary arteries. Ann Biomed Eng 2010; 38:3195–209.

66. Serruys PW, Girasis C, Papadopoulou SL, Onuma Y. Non-invasive fractional flow reserve: scientific basis, methods and perspectives. EuroIntervention 2012;8:511–9.

67. Koo BK, Erglis A, Doh JH, et al. Diagnosis of ischemia-causing coronary stenoses by noninvasive fractional flow reserve computed from coronary computed tomographic angiograms. Results from the prospective multicenter DISCOVER-FLOW (Diagnosis of Ischemia-Causing Stenoses Obtained Via Noninvasive Fractional Flow Reserve) study. J Am Coll Cardiol 2011;58:1989–97.

68. Min JK, Leipsic J, Pencina MJ, et al. Diagnostic accuracy of fractional flow reserve from anatomic CT angiography. JAMA 2012;308:1237–45.

69. Norgaard BL, Leipsic J, Gaur S, et al. Diagnostic performance of noninvasive fractional flow reserve derived from coronary computed tomography angiography in suspected coronary artery disease: the NXT trial (Analysis of Coronary Blood Flow Using CT Angiography: Next Steps). J Am Coll Cardiol 2014;63:1145–55.

70. Baumann S, Wang R, Schoepf UJ, et al. Coronary CT angiography-derived fractional flow reserve correlated with invasive fractional flow reserve measurements—initial experience with a novel physician-driven algorithm. Eur Radiol 2015;25:1201–7.

71. Coenen A, Lubbers MM, Kurata A, et al. Fractional flow reserve computed from noninvasive CT angiography data: diagnostic performance of an on-site clinician-operated computational fluid dynamics algorithm. Radiology 2015;274:674–83.

72. Park HB, Heo R, OH B, et al. Atherosclerotic plaque characteristics by CT angiography identify coronary lesions that cause ischemia: a direct comparison to fractional flow reserve. J Am Coll Cardiol Img 2015;8:1–10.

73. Kristensen TS, Engstrom T, Kelbaek H, von der Recke P, Nielsen MB, Kofoed KF. Correlation between coronary computed tomographic angiography and fractional flow reserve. Int J Cardiol 2010;144:200–5.

74. Park SJ, Kang SJ, Ahn JM, et al. Visual-functional mismatch between coronary angiography and fractional flow reserve. J Am Coll Cardiol Intv 2012;5:1029–36.

75. Budoff MJ, Shaw LJ, Liu ST, et al. Long-term prognosis associated with coronary calcification: observations from a registry of 25,253 patients. J Am Coll Cardiol 2007;49: 1860–70.

76. Bittencourt MS, Hulten E, Ghoshhajra B, et al. Prognostic value of nonobstructive and obstructive coronary artery disease detected by coronary computed tomography angiography to identify cardiovascular events. Circ Cardiovasc Imaging 2014;7:282–91.

77. Mushtaq S, De Araujo Goncalves P, Garcia-Garcia HM, et al. Long-term prognostic effect of coronary atherosclerotic burden: validation of the computed tomography-Leaman score. Circ Cardiovasc Imaging 2015;8:e002332.

78. Garcia-Garcia HM, Serruys PW, Campos CM, et al. Assessing bioresorbable coronary devices: methods and parameters. J Am Coll Cardiol Img 2014;7:1130–48.

79. Wong DT, Ko BS, Cameron JD, et al. Comparison of diagnostic accuracy of combined assessment using adenosine stress computed tomography perfusion + computed tomography angiography with transluminal attenuation gradient + computed tomography angiography against invasive fractional flow reserve. J Am Coll Cardiol 2014;63:1904–12.

80. Hell MM, Dey D, Marwan M, Achenbach S, Schmid J, Schuhbaeck A. Non-invasive prediction of hemodynamically significant coronary artery stenoses by contrast density difference in coronary CT angiography. Eur J Radiol 2015;84: 1502–8.

81. Wang R, Renker M, Schoepf UJ, et al. Diagnostic value of quantitative stenosis predictors with coronary CT angiography compared to invasive fractional flow reserve. Eur J Radiol 2015;84: 1509–15.

KEY WORDS cardiac computed tomography, coronary artery disease, functional evaluation